component of the Bloch electric field, as in $\boldsymbol{E}_{kn} = \Sigma_{\boldsymbol{G}} \boldsymbol{e}_{kn\boldsymbol{G}} e^{i(\boldsymbol{k}+\boldsymbol{G})\cdot\boldsymbol{r}}$.
25. A. Yariv, P. Yeh, *Optical Waves in Crystals: Propagation and Control of Laser Radiation* (Wiley, New York, 1984), chap. 6.
26. The contour formed by $\boldsymbol{u}$ is similar to the ray surface in (*29*), though it now represents group velocities of different frequencies.
27. S. G. Johnson, J. D. Joannopoulos, *Opt. Express* **8**, 173 (2001).
28. The simulation uses a thick perfectly matched layer boundary region that overlaps 10 periods of the photonic crystal similar to that used in (*30*) and can absorb the Bloch waves away from a band edge. The moving charge is implemented as a point-like current density that is oriented toward the direction of motion and whose position depends on time.
29. M. Born, E. Wolf, *Principles of Optics: Electromagnetic Theory of Propagation, Interference and Diffraction of Light* (Cambridge Univ. Press, New York, ed. 7, 1999).
30. M. Koshiba, Y. Tsuji, S. Sasaki, *IEEE Microwave Wireless Components Lett.* **11**, 152 (2001).
31. Supported in part by NSF's Materials Research Science and Engineering Center program (grant no. DMR-9400334) and the Department of Defense, Office of Naval Research, Multidisciplinary University Research Initiative program (grant no. N00014-01-1-0803).

18 October 2002; accepted 5 December 2002

A Reversibly Switching Surface

Joerg Lahann,[1] Samir Mitragotri,[2] Thanh-Nga Tran,[1] Hiroki Kaido,[1] Jagannathan Sundaram,[2] Insung S. Choi,[1]* Saskia Hoffer,[3] Gabor A. Somorjai,[3] Robert Langer[1]†

We report the design of surfaces that exhibit dynamic changes in interfacial properties, such as wettability, in response to an electrical potential. The change in wetting behavior was caused by surface-confined, single-layered molecules undergoing conformational transitions between a hydrophilic and a moderately hydrophobic state. Reversible conformational transitions were confirmed at a molecular level with the use of sum-frequency generation spectroscopy and at a macroscopic level with the use of contact angle measurements. This type of surface design enables amplification of molecular-level conformational transitions to macroscopic changes in surface properties without altering the chemical identity of the surface. Such reversibly switching surfaces may open previously unknown opportunities in interfacial engineering.

Interfacial properties, such as wetting behavior, are defined by the molecular-level structure of the surface (*1*). Diverse modification procedures have been used to permanently alter wettability (*2*–*4*). Control of wettability has been recently demonstrated by elegant methods including light-induced (*5*–*6*) and electrochemical surface modifications (*7*–*10*). These systems require chemical reactions in order to control wettability.

We demonstrate an alternative approach for dynamically controlling interfacial properties that uses conformational transitions (switching) of surface-confined molecules. Polymers have been shown to undergo conformational reorientations when changed from one solvent to another (*11*) or from one temperature to another (*12*, *13*) because of phase transitions between a well solvated and a poorly solvated state (*14*). In contrast, our approach maintains the system's environment unaltered (including solvent, electrolyte content, pH, temperature, and pressure) while using an active stimulus, such as an electrical potential, to trigger specific conformational transitions (e.g., switching from an all-trans to a partially gauche oriented conformation; see Fig. 1). Amplification of conformational transitions to macroscopically measurable changes requires synergistic molecular reorientations of ordered molecules. In principle, this is attainable with a single-molecular layer, such as a self-assembled monolayer (SAM) of alkanethiolates on gold (*15*). However, the dense molecular packing in SAMs and the strong interactions between the methylene groups restrict dynamic molecular motions to the outermost atoms (*16*, *17*). All in situ evidence so far indicates that applied electrical potentials have no effect on long-chain alkanethiolate monolayers on gold within the range of chemical stability of the SAM (*18*). In other words, conventional SAMs are too dense to allow conformational transitions and consequently do not allow for switching. To explore SAMs as a model system for switching, we must establish sufficient spatial freedom for each molecule. Once a low-density SAM is created, preferential exposure of either hydrophilic or hydrophobic moieties of the SAM to the surrounding medium could be exploited for the switching of macroscopic surface properties.

(16-Mercapto)hexadecanoic acid (MHA) was chosen as a model molecule because it (i) self-assembles on Au(111) into a monolayer and (ii) has a hydrophobic chain capped by a hydrophilic carboxylate group, thus potentially facilitating changes in the overall surface properties. To create a monolayer with sufficient spacing between the individual MHA molecules, we used a strategy that exploits synthesis and self-assembly of a MHA derivative with a globular end group, which results in a SAM that is densely packed with respect to the space-filling end groups but shows low-density packing with respect to the hydrophobic chains. Subsequent cleavage of the space-filling end groups establishes a low-density SAM of MHA. The spatial dimensions of the precursor molecule to be used were adapted to match the optimum alkanethiolate density for conformational rearrangements.

The equilibrium low-energy conformational state of each of the sparsely packed MHA

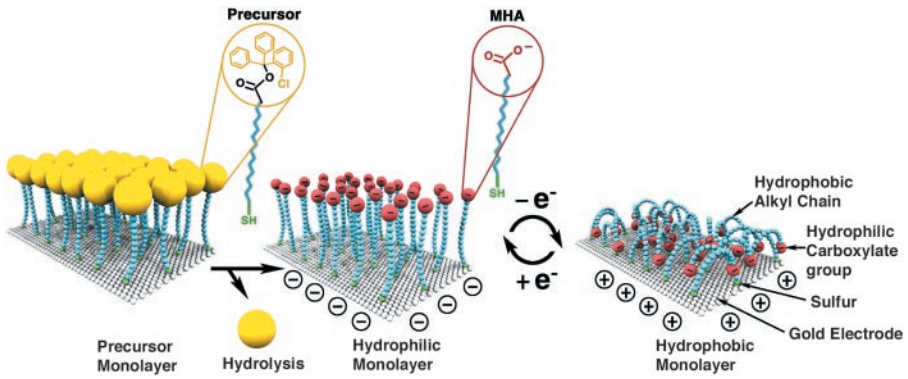

Fig. 1. Idealized representation of the transition between straight (hydrophilic) and bent (hydrophobic) molecular conformations (ions and solvent molecules are not shown). The precursor molecule MHAE, characterized by a bulky end group and a thiol head group, was synthesized from MHA by introducing the (2-chlorophenyl)diphenylmethyl ester group.

[1]Department of Chemical Engineering, Massachusetts Institute of Technology (MIT), 45 Carleton Street, Cambridge, MA 02139, USA. [2]Department of Chemical Engineering, University of California at Santa Barbara, Santa Barbara, CA 93106, USA. [3]Department of Chemistry, University of California at Berkeley, Material Science Division, Lawrence Berkeley Laboratory, Berkeley, CA 94720, USA.

*Present address: Department of Chemistry and School of Molecular Science (BK21), Korean Advanced Institute of Science and Technology, Daejeon 305-701, Korea.

†To whom correspondence should be addressed. E-mail: rlanger@mit.edu

molecules is all trans (all C-C-C-C torsion angles of the hydrophobic core are 180 degrees) (*15*). Upon applying an electrical potential, the negatively charged carboxylate groups experience an attractive force to the gold surface, causing the hydrophobic chains to undergo conformational changes. This chain bending disrupts the all-trans conformational state and causes the aliphatic MHA chains to adopt a mixture of trans and gauche conformations. Thus, the "bent" state of the MHA chains is characterized by an ensemble of molecules in mixed conformations, which maximizes the intermolecular van der Waals contact, and exposes the hydrophobic chains of the MHA molecules to the surrounding medium. To obtain a theoretical estimate of the packing density that would provide sufficient conformational freedom for optimal arrangement of the bent states of the MHA molecules, we performed molecular simulations of MHA monolayers, computing intramolecular bonded interactions and inter- and intramolecular nonbonded interactions. Simulations were conducted starting from assemblies of MHA molecules in bent states. Six assemblies with area-per-molecule values in the range between 0.29 and 2.59 nm^2 were studied (Materials and Methods). For small area-per-molecule values, relaxation of the highly constrained assemblies was dominant resulting in a steep decline of the potential energy as S-S spacings were widened. The plot of potential energy versus area per molecule (Fig. 2) shows that steric constraints are reasonably low for area-per-molecule values of 0.65 nm^2 or higher. On the other hand, the spacing between the MHA molecules for an area-per-molecule value of 0.65 nm^2 still permits a substantial overlap of MHA molecules, leading to favorable hydrophobic interactions between alkyl chains. Thus, even for the system with the widest S-S spacing of 1.73 nm, sufficient overlap of neighboring chains occurred and prevented the overall energy of the system from approaching zero. We conclude from these simulations that an area-per-molecule of 0.65 nm^2 is optimum because it supports steric relaxation and allows for substantial chain overlap.

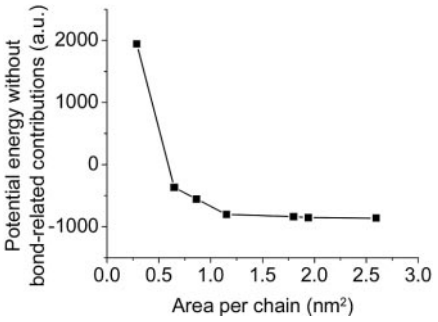

Fig. 2. Nonbonded interaction energy of MHA molecules versus area per molecule. a.u., arbitrary units. To evaluate the effect of the packing density on the conformational transitions and steric interactions of the MHA molecules, we chose as a starting point an assembly of 64 alkanethiolates that were forced into a bent molecular state (distance between sulfur and carbonyl carbon below 0.4 nm). Electrostatics were ignored because the goal of this simulation was to estimate the optimal geometrical spacing between the MHA molecules to allow for conformational transitions that provide switching capabilities to the monolayer. Nearest neighbor distances were set to be between 0.58 and 1.73 nm (*35*). A distance of 0.58 nm between two sulfur atoms corresponds to the densest packing we could establish with a bent assembly, and the distance of 1.73 nm was chosen as an upper limit to guarantee chain-chain overlap (an all-trans oriented chain of MHA has an approximate length of 2.24 nm). All alkanethiolates were confined on a hexagonal gold lattice (Au-Au distance of 0.29 nm), and sulfur and gold atoms were fixed in space. The intermolecular potential was adopted from (*36*, *37*), and the potential describing the interactions between carbon and sulfur atoms with the gold surface was selected to mimic the values reported by Hautman and Klein (*38*).

On the basis of these theoretical considerations, we synthesized a MHA derivative with a globular end group [(16-mercapto) hexadecanoic acid (2-chlorophenyl)diphenylmethyl ester, MHAE]. Its space-filling end group (about 0.67 nm^2) matched closely with the previously determined area of 0.65 nm^2. Self-assembly of MHAE on gold and subsequent removal of the acid-labile end groups resulted in a low-density SAM of MHA (*19*). The quantitative removal was verified by the absence of the signal of chlorine as detected by x-ray photoelectron spectroscopy (XPS). In addition, the characteristic signal of the Cl-triphenyl ester group at 1743 cm^{-1} in the infrared (IR) spectrum was no longer observed, and the characteristic C=O peak appeared (*20*). We then exposed a low-density SAM of MHA to a solution of *n*-butanethiol immediately after cleavage of the bulky end group and conducted electrochemical desorption. For this mixed SAM, a single desorption peak was detected (orange line in fig. S1). In contrast, two desorption peaks were found for phase-separated SAMs composed of MHA and *n*-butanethiol formed via co-adsorption (blue line in fig. S1), corresponding to the coexistence of two distinct phases (*21*). We conclude from this experiment that preparation of a SAM following the previously mentioned strategy resulted in a rather homogeneously distributed monolayer and not a phase-segregated system. These results support the assumption that the low-density SAM consists of molecules that show increased spacing between individual molecules; the formation of MHA clusters is less likely.

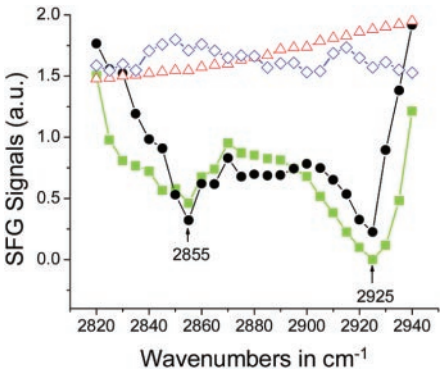

Fig. 3. In situ SFG spectra of the CH-stretch region (2820 to 2940 cm^{-1}) for the low-density SAM exposed to air (green squares), d^3-acetonitrile (red triangles), d^2-water (blue diamonds), and d^8-toluene (black circles). Tunable mid-IR light (1400 to 4000 cm^{-1}) was generated by difference frequency mixing of near-IR light with the fundamental beam of the neodymium: yttrium-aluminum-garnet (Nd:YAG) pump laser in a $LiNbO_3$ or $AgGaS_2$ crystal. The near-IR light was produced through optical parametric generation and amplification of 532-nm light in angle-tuned barium borate crystals. The IR and visible beams were incident on the liquid-solid interface at 40° and 35° and have energy densities of 4 mJ cm^{-2} and 15 mJ cm^{-2}, respectively. SFG spectra were an average of 10 scans with 5 cm^{-1} resolution. SFG signals were collected for 1 to 5 s at every 5 cm^{-1} interval. SFG data were normalized with respect to the reflected IR beam from the electrode to ensure that no false SFG peaks were observed due to strong IR absorption by the thin film of electrolyte above the electrode surface. The lines are drawn as a guide to the eye.

Before examining whether the low-density SAM of MHA undergoes conformational transitions in response to electric potentials, we confirmed the conformational freedom of the alkanethiolates by studying their response to changes in the chemical environment. Sum-frequency generation (SFG) spectroscopy was used for this purpose because it exploits a highly surface-sensitive nonlinear optical process (*22*). The intensity of a peak in the SFG spectrum is affected by the orientation of the adsorbed molecules. An ordered monolayer of all-trans oriented molecules is locally centrosymmetric and hence, by rule of mutual exclusion, its methylene modes are sum-frequency inactive. Gauche conformations break the local symmetry and give rise to SFG signals of the methylene groups (*23*). Figure 3 shows SFG spectra of the low-density SAMs of a MHA that was deprotonated. When exposing the low-density SAM to an apolar medium such as air or toluene, the molecules were found to be in disordered conformations. This state was characterized by the presence of gauche conformations as indicated by SFG signals of the methylene groups at wavelengths of 2925 and 2855 cm^{-1} (Fig. 3, green and black lines). When the same surface was brought in contact with a polar environment (acetonitrile or water), molecules straightened up, presumably by exposing their polar end groups to the solvent. SFG signals associated with the methylene groups were no longer detected. For the dense SAM of MHA, structural reorganizations were far less pronounced and were com-

parable to reported studies (*24*). On the basis of the detected conformational transitions in response to changes in the polarity of the surrounding medium, we conclude that only the low-density SAM provided sufficient chain mobility to allow conformational reorientations from a hydrophilic (straight chains) to a hydrophobic (bent chains) state.

We next assessed switching induced by an active stimulus, such as application of an electrical potential. Information regarding the prospective range of the electrical potential for switching may be obtained from basic energy considerations. First, alkanethiolates adsorbed on gold and exposed to a surrounding solution show electrochemical stability only in a relatively narrow range of electrical potential [–1.046 V to +654 mV with respect to (w.r.t.) the standard calomel electrode (SCE)] (*25*). Applied electrical potentials must be within this range of stability. Second, the change in Gibbs free energy of the system must be negative for a change in the monolayer structure to occur. With the use of a basic model, we estimated a potential above about +150 mV (–118 mV w.r.t. SCE) to be required to satisfy the conditions of molecular reorientation in a low-density SAM (*26*).

A SFG spectrometer equipped with an electrochemical quartz cell (*27*) was used to assess the switching of the surface in response to electrical potentials (Fig. 4, A and B). Without applied electrical potential, the SFG spectra recorded in acetonitrile [0.1 M cesium trifluoromethanesulfonate (CT)] were featureless in the range between 2820 and 2940 cm^{-1}, signifying straight molecular conformations of an all-trans orientation. Slightly positive polarization of the gold surfaces (+25 mV w.r.t. SCE), however, initiated simultaneous switching of the molecules indicated by characteristic methylene modes at wavelengths of 2855 and 2925 cm^{-1} (Fig. 4A). The presence of gauche conformations in the molecules implies that the molecules bend their negatively charged end groups toward the positively charged gold surface (Fig. 1). After the positive potential was turned off, the low-density SAM returned to an assembly of straight molecules with all-trans orientation, because SFG signals of the methylene groups were no longer detected. Switching was reversible, with intensities of the SFG signals being nearly constant as the electrical potential was repeatedly applied. In contrast, the dense SAM of MHA did not show reorientations induced by an applied electrical potential, because the SFG signals remained unaltered when potential was applied (Fig. 4B).

We then addressed the question of whether the observed rearrangements could be amplified into macroscopically detectable changes in surface properties. Advancing (open symbols) and receding (solid symbols) contact angles for the low-density (Fig. 4C) and the dense (Fig. 4D) SAMs were determined while applying either +80 or –300 mV w.r.t. SCE between the underlying gold electrode and a platinum-made microelectrode. Four subsequent switch cycles were examined, and contact angles with an aqueous solution were measured. Figure 4C indicates switching of the receding contact angles as the surface polarization was alternately changed. Although the advancing contact angle was independent from the applied potential, the receding contact angle showed a sharp step whenever the polarization of the surface was changed (Fig. 4C, solid squares). The large hysteresis in contact angle can be caused by surface roughness or chemical heterogeneity of the surface (*28*). Because scanning force microscopy did not reveal notable differences in surface roughness between systems configured of molecules in bent and straight states (*29*), the assumption of a chemical discontinuity along the solid-air-liquid contact line best explains the large hysteresis in contact angles and the pronounced sensitivity of the receding contact angle. Following Good and Neumann's wettability model (*30*), the system reflects the behavior of a smooth but chemically heterogeneous system that is composed of a low-energy area (exposed to air) and a high-energy area (exposed to solution). The observed changes in receding contact angle then signify molecular transitions at the high-energy area. SFG results support this assumption (Fig. 3). The drop in contact angle was a reversible phenomenon, because the assembly was switched several times between its hydrophilic (straight molecules) and hydrophobic (bent molecules) state (four times for the study shown in Fig. 4C). In contrast, switching was not observed for the dense SAM (Fig. 4D). We excluded the possibility of electrochemically induced protonation, because it would affect both dense and low-density SAMs similarly (in addition, experiments were conducted at pH = 11.5 to avoid protonation). The applied electrical potentials were well above the estimated lower limit of electrical potentials that permits conformational transitions (*26*) but low enough to be within the potential window of greatest stability for SAMs of alkanethiolates on gold (*25*, *31*). Thus, electrochemical reactions can be excluded as driving forces for the observed changes in surface properties. We conclude that the observed switching in surface properties is microscopically driven by conformational transitions.

This study demonstrates reversible control of surface switching for a low-density monolayer. Because of synergistic molecular reorientations, amplification into macroscopic changes in surface properties is observed. Future research might be directed toward enhancement of macroscopic effects and development of alternative stimuli. The fact that controlled conformational reorientations of single-layered molecules induced observable changes in wettability suggest that these findings may, with further study, have implications in dynamic regulation of macroscopic properties, such as wettability, adhesion, friction, or biocompatibility. Potential applications might include microfluidics, microengineering of smart templates for bioseparation or data storage, or microfabrication of controlled-release devices.

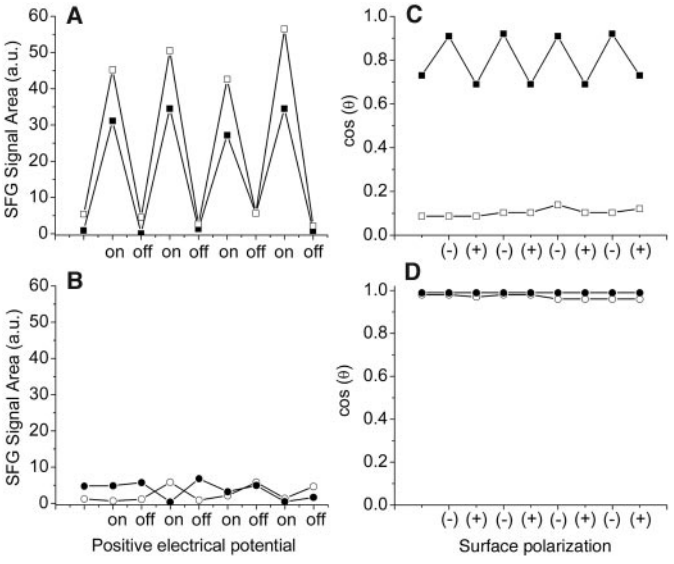

Fig. 4. Microscopic and macroscopic responses of the low-density SAM to an electrical potential as monitored by SFG spectroscopy and contact angle measurements. Relative SFG intensities (peak areas) of the methylene modes at wavelengths of 2855 cm^{-1} (solid symbols) and 2925 cm^{-1} (open symbols) are shown for the low-density (**A**) and the dense (**B**) SAMs measured in d^3-acetonitrile (0.1 M CT) when a potential of +25 mV w.r.t. SCE was repeatedly applied to the system. Cosine of the advancing (open symbols) and receding (solid symbols) contact angles for the low-density (**C**) and the dense (**D**) SAMs were determined while applying either +80 or –300 mV w.r.t. SCE to the underlying gold electrode. Four switch cycles were conducted, and contact angles were measured with an aqueous solution (0.1 M CT, pH = 11.5) at air using a goniometer (VCA-2500XE, Advanced Surface Technology) equipped with an electrometer (6517A, Keithley Instruments) and platinum and carbon fiber microelectrodes (Kation Scientific). Contact angles averaged at least 100 data points from nine samples with maximum errors of ±3°. The SAMs were examined for chemical integrity and deprotonation by IR spectroscopy after an electrical potential was applied. The lines are drawn as a guide to the eye.

References and Notes

1. P. G. deGennes, *Rev. Mod. Phys.* **57**, 827 (1985).
2. G. M. Whitesides, P. E. Laibinis, *Langmuir* **6**, 87 (1990).
3. P. E. Laibinis, C. D. Bain, R. G. Nuzzo, G. M. Whitesides, *J. Phys. Chem.* **99**, 7663 (1995).
4. M. K. Chaudhury, G. M. Whitesides, *Science* **256**, 1539 (1992).
5. S. Abbott, J. Ralston, G. Reynolds, R. Hayes, *Langmuir* **15**, 8923 (1999).
6. K. Ichimura, S.-K. Oh, M. Nakagawa, *Science* **288**, 1624 (2000).
7. N. L. Abbott, C. B. Gorman, G. M. Whitesides, *Langmuir* **11**, 16 (1995).
8. M. Byloos, H. Al-Maznai, M. Morin, *J. Phys. Chem. B* **105**, 5900 (2001).
9. A. Iannelli, J. Merza, J. Lipkowski, *J. Electroanal. Chem.* **376**, 49 (1994).
10. B. S. Gallardo *et al.*, *Science* **283**, 57 (1999).
11. M. D. Wilson, G. M. Whitesides, *J. Am. Chem. Soc.* **110**, 8718 (1988).
12. G. De Crevoisier, P. Favre, J. Corpart, L. Leibler, *Science* **285**, 1246 (1999).
13. Y. G. Takei *et al.*, *Macromolecules* **27**, 6163 (1994).
14. T. P. Russell, *Science* **297**, 964 (2002).
15. Y. Xia, G. M. Whitesides, *Angew. Chem. Int. Ed.* **37**, 550 (1998).
16. M. H. Schoenfisch, J. E. Pemberton, *Langmuir* **15**, 509 (1999).
17. R. Anderson, M. Gatin, *Langmuir* **10**, 1638 (1994).
18. M. A. Hines, J. A. Todd, P. Guyot-Sionnest, *Langmuir* **11**, 493 (1995).
19. A low-density monolayer was prepared by (i) immersing Au(111) in a solution of MHAE (1mM, in ethanol; refer to Materials and Methods for details regarding the synthesis of MHAE) and (ii) removing the acid-labile end group by incubation in trifluoroacetic acid (40% in ethanol). The thickness of the SAM of MHAE was 2.05 ($\pm$0.1) nm as examined by ellipsometry. Formation of islands of adsorbed thiolates was ruled out by cyclic voltammetry (Gamry PC4-300 potentiostat; polycrystalline Au counter and Ag-AgCl reference electrodes; scan rate, 50 mV s^{-1}; 10 cycles; scan range, –0.2 to 0.5 V w.r.t. Ag-AgCl), revealing a shielding of the gold surface by the SAM of MHAE that was comparable to dense SAMs (*32*).
20. In air, the low-density monolayer collapsed into a disordered configuration with a thickness of 1.1 ($\pm$0.1) nm as confirmed by ellipsometry. This value was significantly lower than the thickness of a dense SAM [2.03 ($\pm$0.1) nm] and indicated the loss of two-dimensional order due to increased spacing between the adsorbed molecules. The collapsed structure was also characterized by IR spectroscopy, which revealed general features of a disordered monolayer, such as the red shift of the methylene bands from 2921 and 2852 cm^{-1} (dense SAMs of MHA) to 2929 and 2858 cm^{-1}. Furthermore, we detected an increased static contact angle with water of 62° as compared to 10° measured for the dense SAMs of MHA. The carboxylic acid group was deprotonated under argon atmosphere by incubation with a degassed aqueous cesium hydroxide solution (0.1 M), and completeness was verified by IR spectroscopy (BioRad FTS 175, grazing angle of 80°), revealing the absence of the carbonyl signals at 1742 and 1716 cm^{-1} and the presence of signals at 1550 and 1440 cm^{-1}. The low-density SAM showed chemical stability because it remained unaltered after exposure to ambient conditions for 4 weeks (confirmed by XPS and IR spectroscopy).
21. K. Shimazu, T. Kawaguchi, T. Isomura, *J. Am. Chem. Soc.* **124**, 652 (2002).
22. Y. R. Shen, *Nature* **337**, 519 (1989).
23. T. H. Ong, P. B. Davies, C. D. Bain, *Langmuir* **9**, 1836 (1993).
24. S. M. Stole, M. D. Porter, *Langmuir* **6**, 1199 (1990).
25. W. R. Everett, I. Fritsch-Faules, *Anal. Chim. Acta* **307**, 253 (1995).
26. In a first-order approximation, we neglected interactions between the gold surface and solvent or electrolyte molecules, implying that their net energetic contributions are comparably small. We then assumed the negatively charged end groups act as dynamically mobile acceptors dictating the molecular reorientations and assumed the change in Gibbs free energy upon transition of the system to an electrified state ($N \rightarrow E$) as follows: $\Delta g_{total}|_{N\rightarrow E} = \Delta g_{int}|_{N\rightarrow E} + \Delta g_{sur}|_{N\rightarrow E} + g_{ele}$ (1) Δg_{int} is the change in the Gibbs free energy associated with internal reorganization of the molecules, Δg_{sur} reflects the intermolecular interactions of the hydrocarbon chains and their interactions with the surrounding solvent molecules, and g_{ele} describes the electrostatic component associated with attractive forces between the gold surface and the carboxylate groups. Because steric hindrance between the chains is minimal in the low-density SAM, gauche conformations associated with chain bending mainly account for Δg_{int}. Δg_{int} can be approximated as $0.9nkT$, with n being the number of gauche-oriented bonds, k being Boltzmann constant, and T being temperature (*33*). Δg_{sur} primarily originates from exposure of methylene groups to the surrounding aqueous environment that were embedded in the hydrophobic environment before application of an electrical potential. This term is approximated by $1.5mkT$, where m is the number of methylene groups exposed to the aqueous surrounding because of application of electric field (*34*). Assuming further that at least two bonds need to be gauche-oriented in order to observe a detectable change in contact angle, the required contribution from the electrostatic field based on Eq. 1 is $|g_{ele}| > 4.8kT$. The electrostatic contribution of the free energy can be approximately described by $e\psi_o$, where e is the electronic charge and ψ_o is the surface potential (*33*).
27. S. Baldelli, N. Markovic, P. Ross, Y. R. Shen, G. Somorjai, *J. Phys. Chem.* **103**, 8920 (1999).
28. Y. L. Chen, A. Helm, J. N. Israelachvili, *J. Phys. Chem.* **95**, 10736 (1991).
29. Scanning force microscopy did not reveal notable differences in surface roughness between systems configured of molecules in bent [root mean square (RMS) roughness = 1.9 nm] and straight (RMS roughness = 1.5 nm) states. The different states were realized by conducting scanning force microscopy of a low-density SAM in toluene and water, respectively. Our experiments indicated that surface roughness is predominately caused by the intrinsic surface roughness of the gold surface (RMS roughness < 2 nm). All RMS values refer to an area of 500 × 500 nm^2. Refer to fig. S2 for detailed information.
30. A. W. Neumann, R. J. Good, *J. Colloid Interface Sci.* **38**, 341 (1972).
31. H. O. Finklea, S. Avery, M. Lynch, T. Furtsch, *Langmuir* **3**, 409 (1987).
32. F. P. Zamborini, R. M. Crooks, *Langmuir* **14**, 3279 (1998).
33. N. Aydogan, B. S. Gallardo, N. L. Abbott, *Langmuir* **15**, 722 (1999).
34. M. H. Abraham, *J. Chem. Soc. Faraday Trans. 1* **80**, 153 (1984).
35. T. Li, I. Chao, Y. Tao, *J. Phys. Chem. B* **102**, 2935 (1998).
36. W. D. Cornell *et al.*, *J. Am. Chem. Soc.* **117**, 5179 (1995).
37. S. J. Weiner *et al.*, *J. Am. Chem. Soc.* **106**, 765 (1984).
38. J. Hautman, M. L. Klein, *J. Chem. Phys.* **91**, 4995 (1989).

39. We thank S. Baldelli, N. Flynn, R. Raman, M. Stevens, and G. Venkataraman for valuable discussions; G. M. Whitesides and J. Israelachvili for insightful comments on the manuscript; P. E. Laibinis for the use of the IR; and the Materials Research Science and Engineering Center shared facilities (MIT) supported by NSF under award DMR-0213282. J.L. thanks the Fonds der Chemischen Industrie, Germany, for a Justus-Liebig fellowship, and T.-N.T. acknowledges support from the Whitaker Foundation. This work was sponsored in part by the U.S. Army Research Office through the Institute for Soldier Nanotechnologies at MIT under contract DAAD-19-02-002 and NIH. The content of the information does not necessarily reflect the position or the policy of the Government, and no official endorsement should be inferred.

Supporting Online Material

www.sciencemag.org/cgi/content/full/299/5605/371/DC1

Materials and Methods

Figs. S1 and S2

1 October 2002; accepted 27 November 2002

Spatiotemporal Coherent Control of Lattice Vibrational Waves

T. Feurer, Joshua C. Vaughan, Keith A. Nelson*

We achieved automated optical control over coherent lattice responses that were both time- and position-dependent across macroscopic length scales. In our experiments, spatiotemporal femtosecond pulse shaping was used to generate excitation light fields that were directed toward distinct regions of crystalline samples, producing terahertz-frequency lattice vibrational waves that emanated outward from their multiple origins at lightlike speeds. Interferences among the waves resulted in fully specified far-field responses, including tilted, focusing, or amplified wavefronts. Generation and coherent amplification of terahertz traveling waves and terahertz phased-array generation also were demonstrated.

Ultrafast optical control over electronic and/or vibrational responses of atoms, molecules, and crystals has advanced dramatically in recent years (*1*–*8*). Experiments in this field have typically been conducted with femtosecond pulse shaping techniques (*9*) for generation of complex excitation light fields that yield specified coherent responses or that manipulate complex phenomena such as photochemical reactions. Typically, these light fields, as well as the material responses generated by them, are specified as a function of time but not of macroscopic spatial location. For ultrafast responses that move coherently across macroscopic distances, more complete optical control over both spatial and temporal evolution requires the use of time- and position-dependent excitation fields. Here we

Department of Chemistry, Massachusetts Institute of Technology, Cambridge, MA 02139, USA.

*To whom correspondence should be addressed.

ERRATUM

post date 9 May 2003

REPORTS: "A reversibly switching surface" by J. Lahann *et al.* (17 Jan. 2003, p. 371). Insung S. Choi's "present address" affiliation should be the Korea Advanced Institute of Science and Technology, not the Korean Advanced Institute of Science and Technology.